



**Politecnico
di Torino**

Politecnico di Torino

INGEGNERIA MECCANICA (MECHANICAL ENGINEERING)

A.a. 2020/2021

10/2021

Simulation of the Cartridges Filters with CFD method

Relatori:

MANES COSTANTINO
STARNONI MICHELE

Candidati:

GUAN LINRUI

CONTENT

Abstract	1
1. Introduction	2
1.1 The background of the coalescing filters	2
1.2 The objects.....	2
1.3 The CFD method.....	4
2. Theoretical background	6
2.1 The turbulence models.....	6
2.2 The porous-jump function	8
2.3 The Discrete Particle Method.....	8
3. Simulations	10
3.1 Determine the suitable turbulence model.....	10
3.2 Create and simulate the air flow through the 4 cartridges filters	14
3.3 The DPM simulation.....	18
4. Conclusions	21
Reference	22

Abstract

Coalescence fibrous filter cartridges are widely utilized in the oil industry to remove hazardous aerosols of lubricating oil from gas streams, which can be potentially dangerous to the human health and the environment. In this Thesis, I present an Eulerian-Lagrange approach to simulate flow and oil transport on real fibrous filter cartridges used in the industry. The flow field is computed by solving the Reynolds-Averaged Navier-Stokes (RANS) equations and the filter cartridge is modelled as a porous boundary condition. Next, oil particles are injected into the filter cartridge and the location where the particles cross the filter surface is recorded. This thesis has two objectives. The first one is to determine the most appropriate turbulence model to simulate the flow processes happening inside the cartridge. This is done by using a simple geometry with only one cartridge and considering three commonly used turbulence models (namely k- ϵ standard, k- ϵ realizable, and k- ω SST). Calculated values of the pressure drop between the inlet and outlet are then compared to available experimental data for different flowrates in order to determine the most suitable turbulence model. The second goal is to study real operating conditions consisting of four cartridges working in parallel. To this end, two cartridge geometries are used: one symmetric and one asymmetric. After computation of the flow field, oil droplets are injected into the filter cartridge and the oil mass distribution in each of the four cartridges is calculated, with the purpose of determining whether the oil distribution is uniformly distributed along the four cartridges or not, for both configurations.

1. Introduction

1.1 The background of the coalescing filters

Coalescence filters are widely used to remove droplet aerosols such as oil mist from air. They typically consist of multiple layers of fibrous media, which can be wettable (“oleophilic”) or non-wet table (“oleophobic”). Oil mist is emitted by air compressors and engine crankcases in the size range of about 0.1–1 μ m. The aerosol is removed quite efficiently by such filter media, often within the first few layers, and collects on the fibers, where it coalesces with time into much larger drops (Kampa et al., 2014).

It is important to analysis the flow filed in the filters. For the reason, gain the knowledge, to explore the processes, to determine permeability, to determine pressure drop, filtration efficiency without spending lots of money in experiments.

1.2 The objects

This paper has two goals. The first one is to determine the most appropriate turbulence model to simulate the flow processes happening inside the cartridge. This is done by using a simple geometry with only one cartridge and considering three commonly used turbulence models (namely k- ϵ standard, k- ϵ realizable, and k- ω SST). Calculated values of the pressure drop between the inlet and outlet are then compared to available experimental data for different flowrates in order to determine the most suitable turbulence model. The second goal is to study real operating conditions consisting of four cartridges working in parallel. To this end, two cartridge geometries are used: one symmetric and one asymmetric. After computation of the flow field, oil droplets are injected into the filter cartridge and the oil mass distribution in each of the four cartridges is calculated, with the purpose of determining whether the oil distribution is

uniformly distributed along the four cartridges or not, for both configurations.

The first goal can be achieved by simulating the air flow of 5 (100 m³/h, 200 m³/h, 300 m³/h, 400 m³/h, 500m³/h) flow rates through a simple geometry with the 3 turbulence models. The pressure drop is calculated when the simulations have convergence and compared with the experimental data. The whole process is like the Fig 1.1 shows:

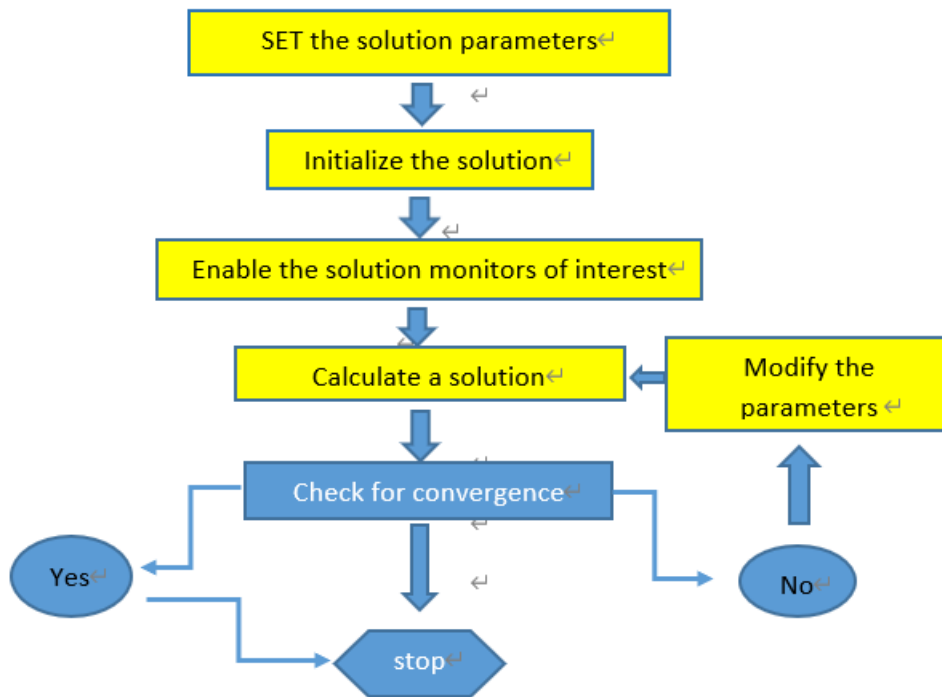


Fig 1.1 The process of the Fluent simulations

The second goal needs two steps. Simulate the air flow of 300m³/h in two 4-cartridges filters (one is symmetric, and one is asymmetric) with the appropriate turbulence model, then use the DPM (Discrete Phase Model) to simulate in the different injection time (5s, 10s, 15, 20s), the oil droplets in the air flow passing through the filters. The oil particle mass distribution normalized to the total mass flow rate can be found in each cartridge to check whether the distributions are even or not.

1.3 The CFD method

There are many partial differential equations in fluid theory, for example, the Reynolds-Averaged Navier-Stokes (RANS) equations, it is difficult to solve them in the conventional method. And it is impossible in practice to investigate the fluid dynamics processes happening inside a filter cartridge using conventional laboratory experiments. To this end, computational fluid dynamics (CFD) can be very helpful for engineers in filter design and optimization, especially in modern days given the constant advances in computer power and software development.”

The core idea for CFD is using discretization methods, such as the finite volume method, to obtain discrete solutions of the governing equations of flow, which to date do not have an exact solution. Grid-based methods consist in dividing the continuum domain into an appropriate number of elements and calculate an approximate solution of the governing partial difference equations in some given points, e.g., the centroids of the elements. Obviously, the greater number of elements, the higher the quality of the approximate solution. In cases where experimental data are available, results of the CFD simulations can be compared and the mesh refined if the match is not satisfactory.

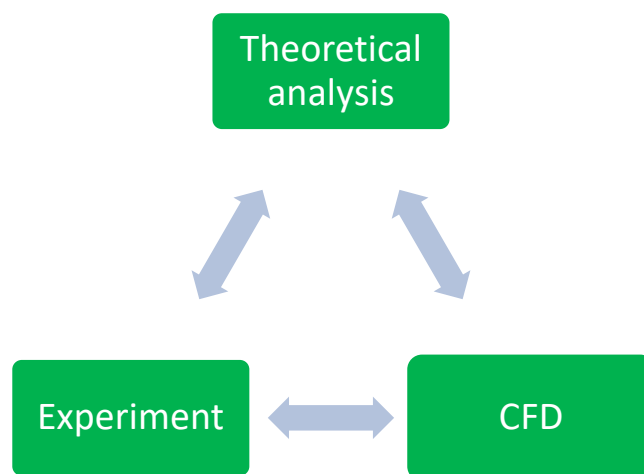


Fig 1.2 The relation between the theory, the experiment and the CFD

The CFD method can be used to solve the problems that the theoretical analysis and experiment are impossible to solve. But the CFD needs the foundation of the theory, and the experiment can verify the results of the CFD method. In the first goal, the pressure drop should be calculated in the CFD process and compared with the experimental data to determine the most suitable turbulence model.

2. Theoretical background

The core idea for the CFD software to solve the fluid mechanics problems is to use the finite volume method (FVM). It is a calculation method for solving partial differential equations numerically. In the finite volume method, the physical entity is divided into grid cells to calculate.

2.1 The turbulence models

The first goal of the simulations is to determine the most suitable turbulence model for the next steps from the three turbulence models (the k- ϵ standard, k- ϵ realizable and k- ω SST models). The pressure drops are calculated only when the residuals of the 6 parameters that the continuity, the velocity of x, y, z directions, the kinetic energy (k), the energy dissipation rate (ϵ and ω) are convergent.

The continuity equation represents the conservation of the mass:

$$\frac{\partial \rho}{\partial t} + \frac{\partial(\rho u_i)}{\partial x_i} = 0 \quad (2.1)$$

In which ρ is the density of the flow, u_i is the velocity for the corresponding direction.

Then the N-S equation is the most important equation for the fluid studies. It shows how the momentum changes in the control volume where need to calculate. For NS equation, its general equation can be written:

$$\frac{\partial u_i}{\partial t} + \sum_j u_j \frac{\partial u_i}{\partial x_j} = -\frac{1}{\rho} \frac{\partial p}{\partial x_i} + \sum_j \frac{1}{\rho} \frac{\partial \tau_{ij}}{\partial x_j} + g_i \quad (2.2)$$

In this equation, p is the pressure, τ_{ij} is the stress tensor, g_i is the external force.

According to the Fluent tutorial guide, the both two k- ϵ turbulences consist of 2 basic equations: the kinetic energy k and the turbulence dissipation ϵ :

$$\frac{\partial(\rho k)}{\partial t} + \frac{\partial(\rho k u_i)}{\partial x_i} = \frac{\partial}{\partial x_i} \left[\frac{\mu_t}{\sigma_k} \frac{\partial k}{\partial x_j} \right] + 2\mu_t E_{ij} E_{ij} - \rho \varepsilon \quad (2.3)$$

$$\frac{\partial(\rho \varepsilon)}{\partial t} + \frac{\partial(\rho \varepsilon u_i)}{\partial x_i} = \frac{\partial}{\partial x_i} \left[\frac{\mu_t}{\sigma_\varepsilon} \frac{\partial \varepsilon}{\partial x_j} \right] + C_{1\varepsilon} \frac{\varepsilon}{k} 2\mu_t E_{ij} E_{ij} - C_{2\varepsilon} \rho \frac{\varepsilon^2}{k} \quad (2.4)$$

u_i is the velocity for the corresponding direction; E_{ij} is the rate of deformation; $\mu_t = \rho C_\mu \frac{k^2}{\varepsilon}$ is the eddy viscosity. The differences between the standard k- ε turbulence model and the realizable one is that C_μ is constant for the standard k- ε turbulence model. The left terms of both 2 equations represent the kinetic energy k and dissipation rate ε change in time plus the transport of k and ε by advection. The right terms are transport and k and ε by diffusion plus the rate of production of k and ε plus the rate of the destruction of k and ε . The k- ε turbulence model is recommended for planar shear layers and recirculating flows. It is very useful for the free-shear layer flows with relatively small pressure gradients and the confined flows where the Reynolds shear stresses are important. And for the Realizable k- ε model, it provides improved solutions for the spreading rate of both planar and round jets. It also exhibits superior performance for flows involving rotation, boundary layers under strong adverse pressure gradients, separation, and recirculation. In virtually every measure of comparison, Realizable k- ε demonstrates a superior ability to capture the mean flow of the complex structures.

By referring to the Fluent tutorial guide, the k- ω SST turbulence model combines the k- ω and the k- ε turbulence models. The first one is used in the inner boundary condition and the latter one is used in the free shear flow. The SST is the short name of the Menter's Shear Stress Transport. The k- ω SST model has a better prediction for the adverse pressure gradients. The equations for the k and ω are:

$$\frac{\partial}{\partial t} (\rho k) + \frac{\partial}{\partial x_i} (\rho k u_i) = \frac{\partial}{\partial x_j} \left(\Gamma_k \frac{\partial k}{\partial x_j} \right) + G_k - Y_K + S_k \quad (2.5)$$

$$\frac{\partial}{\partial t} (\rho \omega) + \frac{\partial}{\partial x_i} (\rho \omega u_i) = \frac{\partial}{\partial x_j} \left(\Gamma_\omega \frac{\partial \omega}{\partial x_j} \right) + G_\omega - Y_\omega + S_\omega \quad (2.6)$$

In these equations, G_k represents the generation of turbulence kinetic energy due to mean velocity gradients. G_ω represents the generation of ω . Γ_k and Γ_ω represent the

effective diffusivity of k and ω , respectively. Y_K and Y_ω represent the dissipation of k and ω due to turbulences. The All of the above terms are calculated as described below. S_k and S_ω are user-defined source terms.

2.2 The porous-jump function

For the cartridge filters inside the vessel, the porous-jump type in the FLUENT software can be used for the filters. Its principle is the Darcy's Law:

$$Q = \frac{kA(P_a - P_b)}{\mu L} \quad (2.7)$$

Q is the flow rate through this medium, k is the permeability, A is the cross section of the medium, $(P_a - P_b)$ is the total pressure drop from a side to b side, L is the thickness of this medium, μ is the fluid viscosity.

The pressure gradient $\Delta P = (P_a - P_b)$ is the most important figure for both the simulations and the experiments. The method for choosing the correct turbulence model is comparing all the flow rate pressure gradients of all 3 turbulence models and comparing them to the experiment data.

Furthermore, in the Fluent, an additional inertial loss term is introduced into the formula:

$$\Delta P = -\left(\frac{\mu}{k}v + C_2 \frac{1}{2}\rho v^2\right)L \quad (2.8)$$

Additionally, v is the velocity normal to the porous face, C_2 is the pressure jump coefficient.

2.3 The Discrete Particle Method

DPM is the Discrete Phase Model. It is used for the discrete particle calculation in the simulations. In the case, when the air flow is steady after the residuals have the convergences, the simulation of the injection of particles should begin. It means the air

flow is combined oil droplets like the aerosols in the real environment that pass through the filters (the task is to find out how much oil trapped in the cartridge filters). The injection time decides the total amount of the particles into the filters. Because the process is discrete, the time step needs to be evaluated by the formula:

$$t^* = 0.15 k/\varepsilon \quad (2.9)$$

k is the average volumetric kinetic energy in the 4-cartridge filters geometry.

ε is the average volumetric energy dissipation rate in the 4-cartridge filters geometry.

And the number of the steps:

$$N = t/t^* \quad (2.10)$$

t is the total injection time.

The maximum track step numbers is the max step to track the particles' fate (trapped, reflected, escaped etc.). If its value is too small, the tracks of some particles are incomplete, the results are not credible. The value of it should be estimated by: $N_{max} =$

$$L * N_{CELL}$$

L is the length scale for the simulation, N_{CELL} is the amount of the cells.

3. Simulations

3.1 Determine the suitable turbulence model

This process is that simulates the different flow rates of air (100m³/h, 200 m³/h, 300m³/h, 400m³/h, 500m³/h) passing through the filter geometry. The pressure drop Δp is the index to calculate and compare with the experiment data when the residuals of the 6 parameters (continuity, the velocity of x, y, z directions, the kinetic k and the energy dissipation rate ϵ or ω) are convergent.

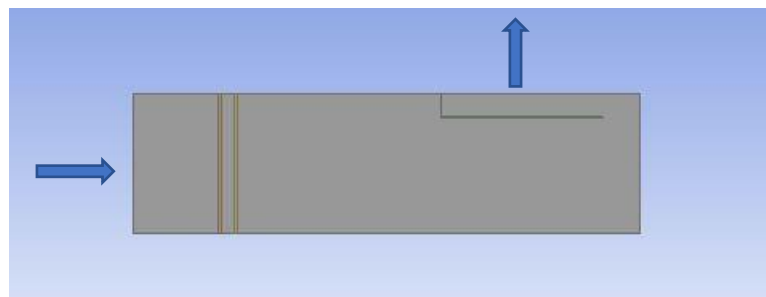


Fig 3.1 The out view of the filter, arrows show the direction of the air flow

The arrows show the positions of the inlet and the outlet of the geometry. The area of the inlet is 0.022698m², the outlet is 0.010207m². The inlet velocities can be estimated by the formula: $V = \frac{Q}{60A}$ [m/s], which are 1.22 m/s, 2.44 m/s, 3.66m/s, 4.88 m/s, 6.10 m/s.

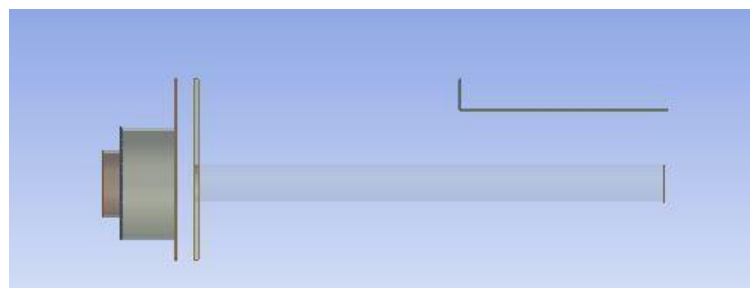


Fig 3.2 The inside construction of the filter

In the **Fig 3.2**, the cylinder is the cartridge filter, the height is the 1.32m.

The mesh is the necessary pre-process of the simulations. The mechanism of the FLUENT solving the fluid problem is FVM (Finite Volume Method), dividing the whole geometry into small cells to approach the exact values for complex constructions. The finer the mesh does, the more elements the project will contain, and the results are more reliable, but it will take more time and consume more CPU sources.

The set-up of the boundary conditions is that the inlet velocity is from 1.22 m/s to 6.10 m/s, the outlet gauge pressure is zero, which means the outlet pressure is the atmosphere pressure. The cartridge-lid should be set as the wall because the top of the cartridge filters is considered that not any flow can penetrate it.

The porous-cartridge part is the part of the filter where the flow passes through. The parameters can be set by according to the Darcy' Law (2.8):

$$\Delta P = -\left(\frac{\mu}{k} v + C_2 \frac{1}{2} \rho v^2\right) L \quad (2.8)$$

the permeability $k=7e-11 \text{ m}^2$ is found by matching the numerical values with the experimental values, the thickness L is 0.025m, due to neglecting the kinetic energy loss in the porous zone, $C_2 = 0$.

The under-relaxation number for the solution control means how much to choose the value changes for the next iterations. For example, if the pressure under-relaxation number set as 0.3, $P_{i+1} = P_i + 0.3 * \Delta P$. The fomula represents that the pressure if the (i+1)th iteration is the ith plus the change, the change value can be adjusted (the under-relaxation number is between 0~1). The larger value if the changes have, the time need for the convergence is small, but the process is more unstable and will get a rougher result. The smaller ones have the opposite effect. For the different simulations the appropriate under-relaxation numbers are necessary.

The residual conditions are the convergence conditions which simulations once reach,

the process is stop. The default values for all 6 residuals are 1×10^{-3} , which are not enough for the simulation results. All of them should be modified to 1×10^{-4} , and the under-relaxation numbers should be carefully chosen because the larger values they have, the more impossible to get the convergence.

According to the FLUENT tutorial guide, the residuals are not the only standard to determine that the results can be trusted. In this simulation, the pressure drop is the index need to be calculated, so the monitor of the inlet pressure can make sure the value of the pressure drop is credible.

Finally, initialize the process. Choose the standard initializing the velocity is relative to the inlet. Then calculate.

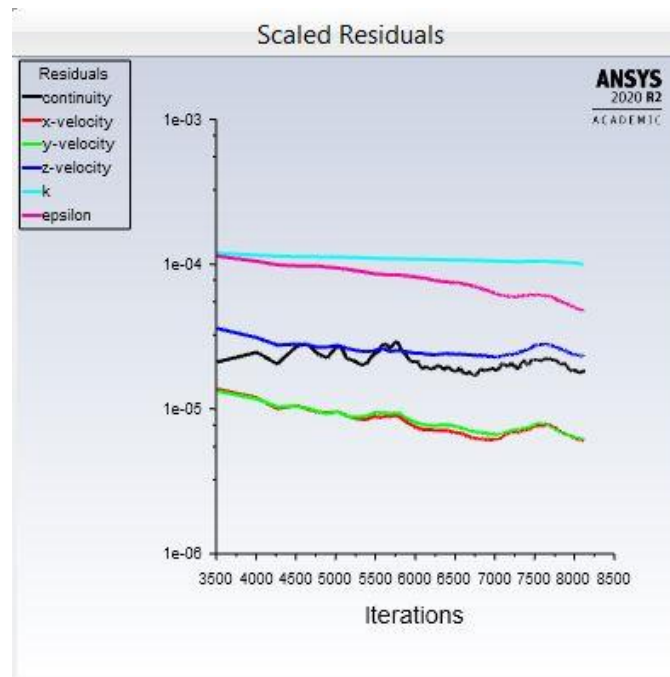


Fig 3.3 The example of the residual plot behavior

The **Fig 3.3** shows that all the 6 residuals are convergent.

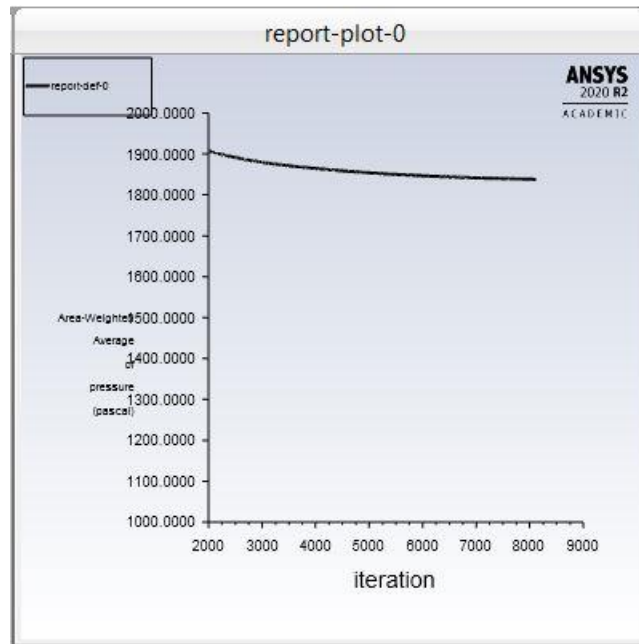


Fig 3.4 The example of the inlet pressure plot

The **Fig 3.4** is the inlet pressure plot. According to the plot, at the 8500 iterations, the inlet pressure is quite steady, and its value is about 18mbar.

The post-process for the simulations is selecting the surface integrals at the report sections. Calculate the inlet and outlet total pressure drop in the averaged-weighted areas. Recalling that the total pressure is the sum of the static pressure and the dynamic pressure.

The groups of all the data of the simulations and experiment are:

Flow rate	V inlet	k-eps real(mabr)	k-eps standard	k-omega SST	experiment
100	1.22	3.45	2.79	2.55	3.94
200	2.44	7.92	6.98	6.13	8.65
300	3.66	13.25	11.84	9.56	14.11
400	4.88	18.33	16.77	14.65	20.22
500	6.10	24.82	21.32	18.69	26.97

Tab 3.1 the pressure drop results

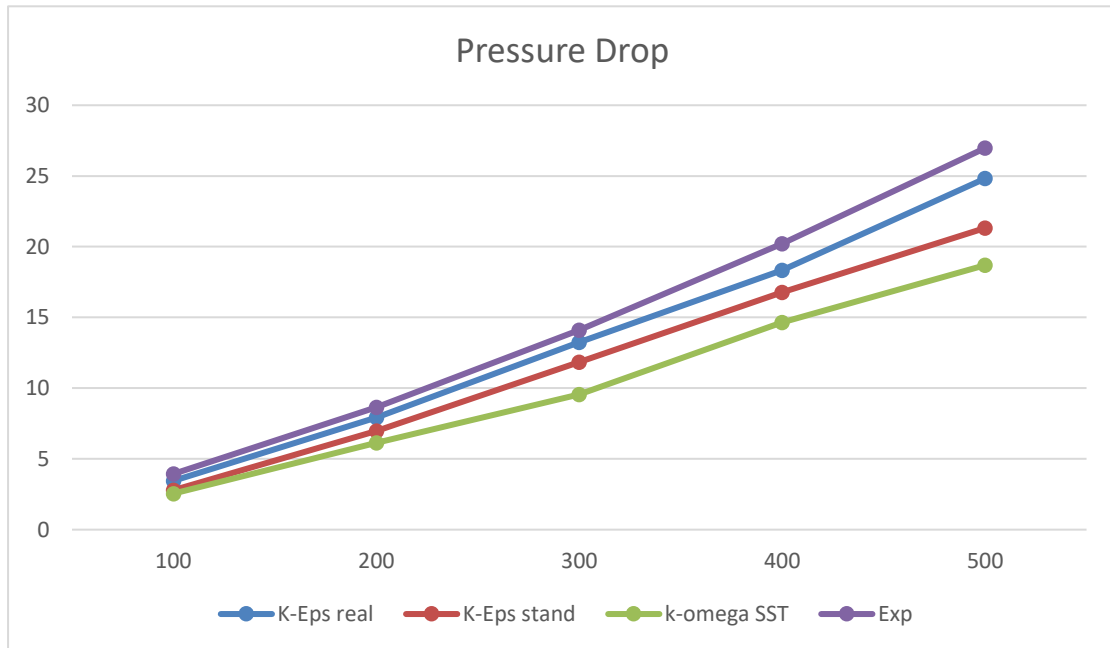


Fig 3.5 The diagram of the pressure drop

The Fig 3.5 shows all the 3 turbulence models results comparing to the experiment data. In the diagram the k- ϵ realizable model is very close to the experiment results than the other 2 models.

The theoretical analysis of the conclusion is that the two k- ϵ models are more suitable for the recirculating flow simulations than the k- ω SST model. Furthermore, the k- ϵ realizable is the most suitable because it is specified from the standard one improving its performance in the rotating flow when it has a strong adverse pressure gradient. But the pressure drop of all the three turbulence models are below the experiment data, the reason is that inertial effects are neglected, the $C_2 = 0$.

3.2 Create and simulate the air flow through the 4 cartridges filters

This paper is to find out how the injection time and the symmetry of the geometries affect the ability of the filters to remove the oil droplets from the air flow. The DPM method can simulate the discrete oil particles in the air flow. Before this process, the

simulation of the air flow is necessary, because when the simulation of the air flow have the convergences, the DPM should begin, and the values of the kinetic energy k and the energy dissipation rate ϵ of the average volume are needed to evaluate the time step of the DPM simulation.

The flow rate of the air flow is $300\text{m}^3/\text{h}$, due to the previous result the most suitable turbulence model of this simulation is the $k\text{-}\epsilon$ realizable model.

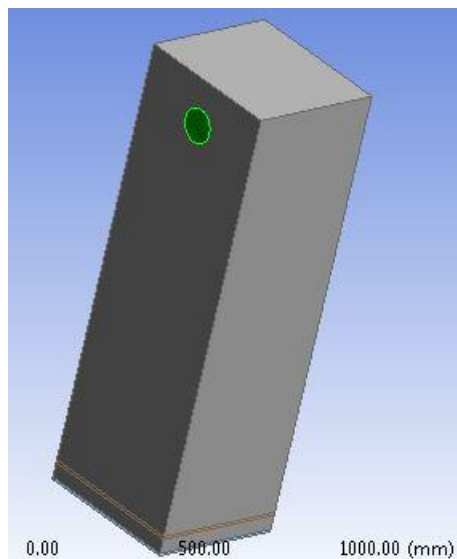


Fig 3.6 The out view of the asymmetric geometry

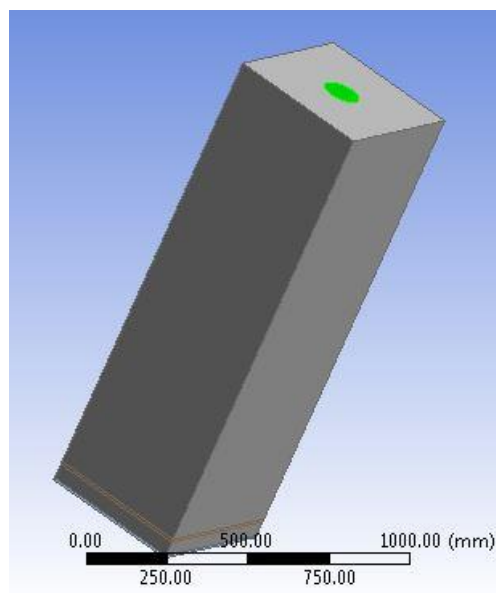


Fig 3.7 The out view of the symmetric geometry

Two geometries are created, they share the same size (the inlet areas are $0.022698m^2$, the outlet areas are $0.010207m^2$), the only difference is that the symmetric geometry has the outlet in the center of the geometry top face as the green area in the **Fig 3.7** and the other one outlet is on the one of the side faces, as the **Fig 3.6** shows.

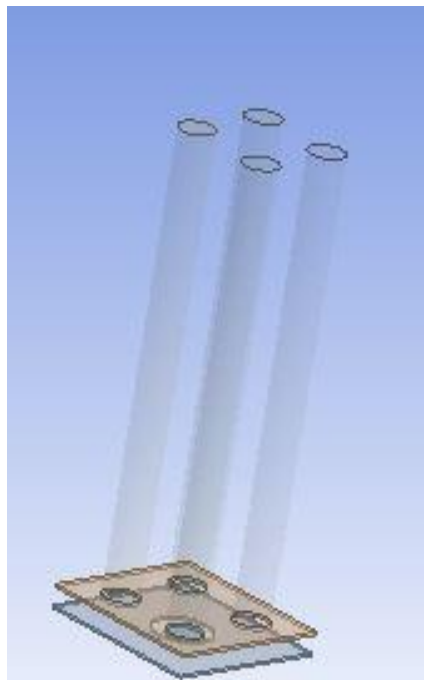


Fig 3.8 The inside constructs of the 2 geometries

The two geometries inside constructs are also the same, the heights of the 4 cylinders are 1.32m.

Then mesh the geometries and get the cell numbers are 1.2 million, which is needed to evaluate the maximum number of steps by $N \geq L * N_{\text{MESH}}$.

According to the flow velocity formula $V = \frac{Q}{60A}$ [m/s], the inlet velocity equals 3.66 m/s for the flow rate $300m^3/h$. The cartridges share the same settings with the previous one. The permeabilities are $7 \cdot 10^{-11}m^2$, the thickness is 0.025m. The residuals are all set as $1e-4$.

Monitor of the inlet pressure, the average volumetric kinetic (k), the average volumetric

energy dissipation rate (ϵ) in the turbulence section is necessary. When the residuals are convergent, the values in the plots of these three parameters should be stable. Initialize and start the simulation. After about 27000 iterations, the residuals have the convergences, if the convergence condition is the default value $1e-3$, the quantities of the average volumetric kinetic (k), the average volumetric energy dissipation rate (ϵ) are wrong. Because when the default conditions are met, the plots are still decreasing, the values of them are not credible. The two geometries have the same behavior of the residual, the inlet pressure, the kinetic and the energy dissipation rate plots. Like the **Fig 3.9**, the **Fig 3.10**, the **Fig 3.11** the **Fig 3.12** show, all the plots are steady.

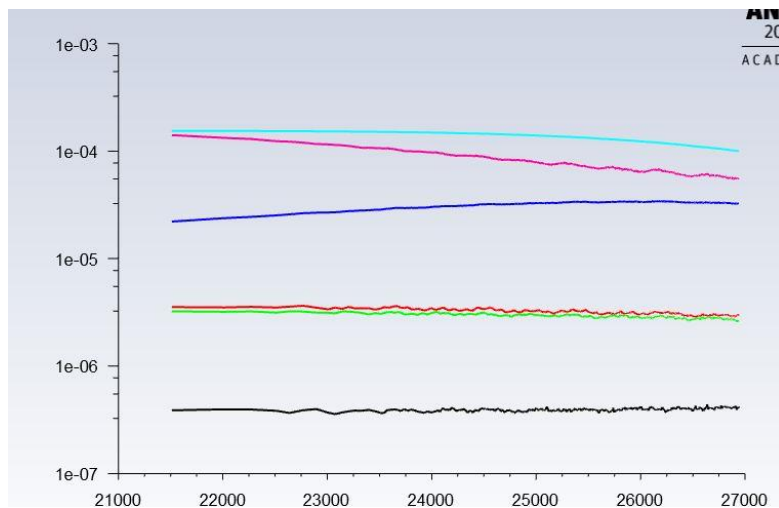


Fig 3.9 The plot of the residuals

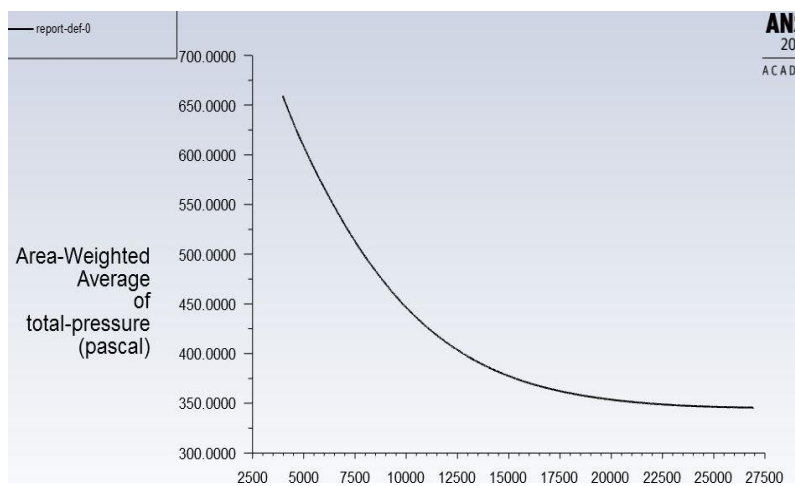


Fig 3.10 The plot of the inlet pressure

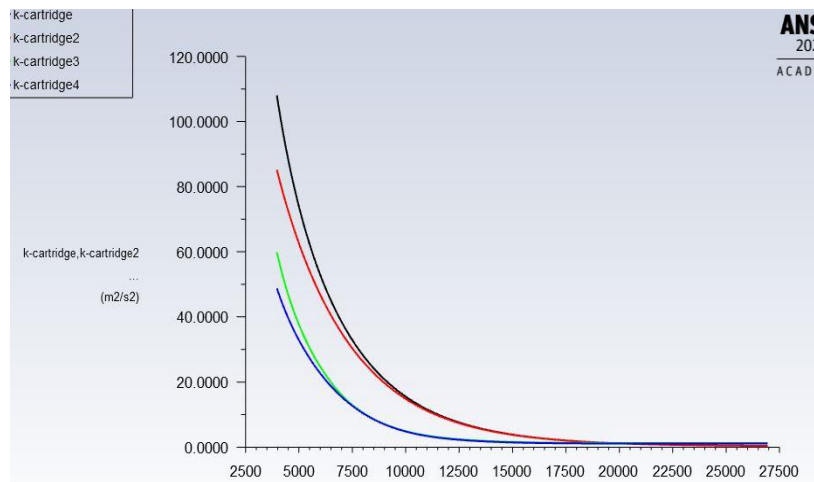


Fig 3.11 The plot of the 4 cartridges kinetic energies

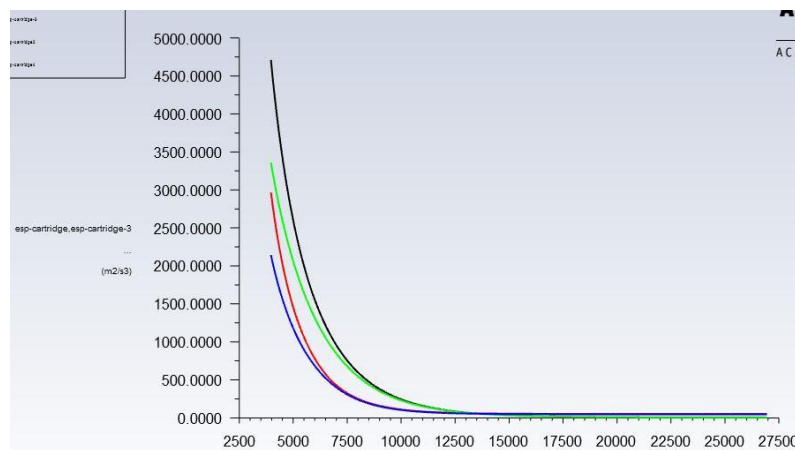


Fig 3.12 The plot of the 4 cartridges dissipation rate

The value of the k is $0.44\text{m}^2/\text{s}^2$ and the value of the ϵ is $9.17 \text{ m}^2/\text{s}^3$.

3.3 The DPM simulation

The DPM (Discrete Particle Model) is the tool commonly used to simulate the discrete particles in the continuous flow. The effect of the injection time and the symmetry of the geometries should be demonstrated by the mass distributions normalized to the total mass flow rate.

The injection time are 5s, 10s, 15s, 20s. The time step can be estimate by the formula:

$$\tau = 0.15k/\epsilon$$

in which the k is the average kinetic energy of the 4 cartridges, the ϵ is the average

volumetric energy dissipation rate. After calculating the τ is 0.00

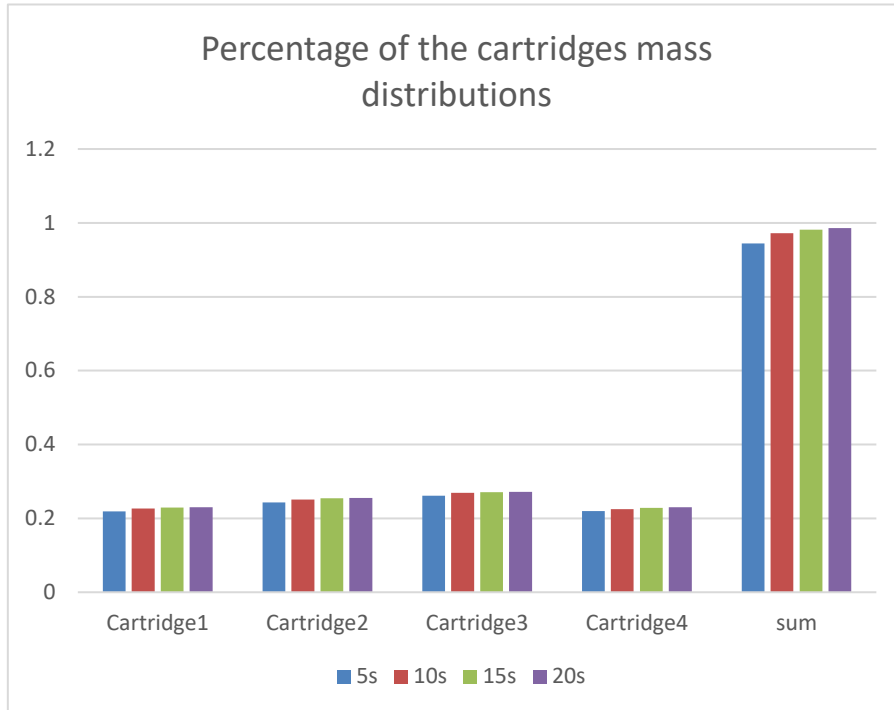
7s. Then the numbers of step can be calculated by: $N = T/\tau$, T is the injection time which are 5s, 10s, 15s, 20s.

The Max. Number of Steps $N \geq L * N_{MESH}$, L is the Step Length Scale, N_{MESH} is the element numbers of the mesh. $N = 7$ million. The DPM iteration interval is 10 which means every 10 iterations the simulation will start an injection. And the injection is just needed to do once.

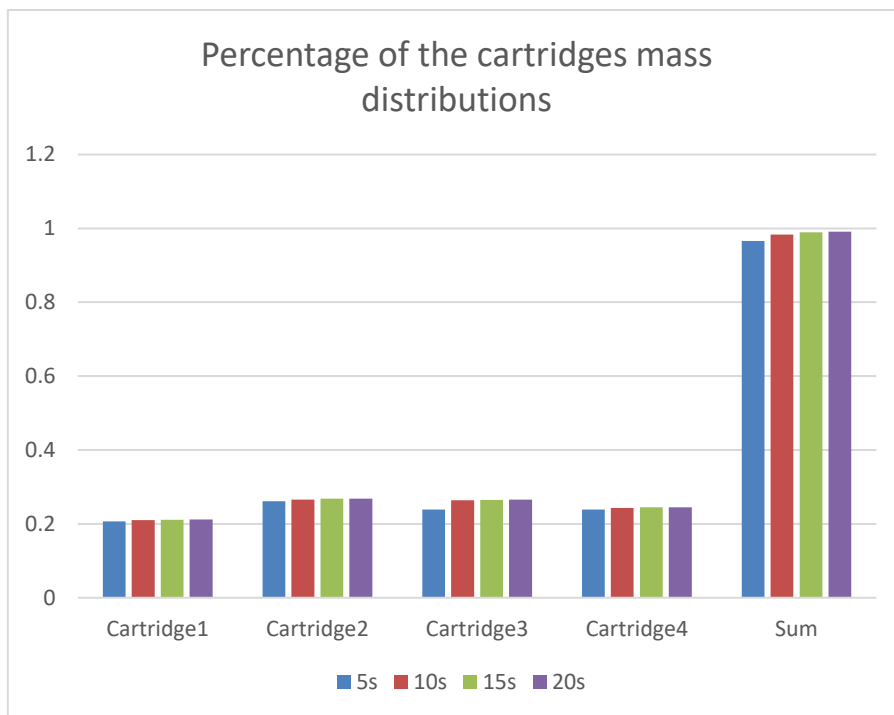
The Saffman lift force option is selected because this form of the lift force is intended for small particle Reynolds numbers and recommended only for submicron particles. The virtual mass force is required to accelerate the fluid surrounding the particle.

The diameter of the particles is 300 nm. The injection surface is at the inlet. The material of the droplets is fuel-oil liquid. The boundary conditions are set as trapped in the 4 cartridges to simulate that the oil droplets are eliminated by the cartridge filters in the real industrial field. The other parts are set as reflect to let the droplets into the cartridges. The turbulence is dispersing discrete random, and the direction of the injection should be normal to the surface of the inlet. The relaxation number of the discrete control is 0 because the injection is only needed to do once. The mass flow rate is 8.334×10^{-5} kg/s and the velocity are 3.66 m/s same as the air flow.

After the DPM process is finished. In the summary of the particle-tracks of the report section, the mass distribution can be calculated.



Tab 3.2 The mass distribution of the symmetric geometry



Tab 3.3 The mass distribution of the asymmetric geometry

The mass distribution of the 4 cartridges inside the symmetrical geometry can be considered as equal, the slight differences may be caused by the meshes difference

which cannot be perfectly divided or due to the turbulence. And with the injection time increasing, the total mass distribution is also increased.

The asymmetrical geometry also has the almost equal mass distribution in the 4 cartridges. The symmetric or asymmetric do not cause obvious differences in the 4 cartridges.

4. Conclusions

According to the comparison between the simulation results and the experimental data, the optimal turbulence for the coalescing filters is the $k-\epsilon$ realizable , but the values of the pressure drop are still lower than the real one. The reason is that the inertia effect is not considered, if the jump coefficient C_2 is set, the result is closer.

When the injection time increases from 5s to 20s, the percentage of the mass distribution of each cartridge is rising, and the sum of them also ascents.

The mass distribution of each cartridge in the symmetric and asymmetric geometries are almost the same. The slight difference may be caused by the meshes and the turbulence.

Reference

- [1] Pietro Asinari, Eliodoro Chiavazzo (2013). An Introduction to Multiscale Modeling with Applications. *Esculapio Press*.
- [2] B. Andersson, R. Andersson, L. Hakansson, M. Mortensen etc (2012). Computational Fluid Dynamics for Engineers. *Cambridge Press*.
- [3] The Ansys Company. Fluent Tutorial Guide 2020.
- [4] Lin Jianzhong (2013). Fluid Mechanics. *Tsinghua University Press*.
- [5] Kampa, D., Wurster, S., Buzengeiger, J., Meyer, J., & Kasper, G. (2014). Pressure drop and liquid transport through coalescence filter media used for oil mist filtration. *International journal of multiphase flow*, 58, 313-324.
- [6] Mead-Hunter, R., King, A. J., & Mullins, B. J. (2014). Aerosol-mist coalescing filters—A review. *Separation and Purification Technology*, 133, 484-506.
- [7] Liu, Z., Ji, Z., Wu, X., Ma, H., Zhao, F., & Hao, Y. (2016). Experimental investigation on liquid distribution of filter cartridge during gas-liquid filtration. *Separation and Purification Technology*, 170, 146-154..